Periodic orbits in a near Yang-Mills potential

G. Contopoulos and M. Harsoula

Research center for Astronomy and Applied Mathematics, Academy of Athens, Soranou Efessiou 4, 115 27 Athens, Greece

E-mail: mharsoul@academyofathens.gr ‡; gcontop@academyofathens.gr;

February 2023

Abstract.

We study numerically the orbits in the Yang-Mills (YM) potential $V = \frac{1}{2}x^2y^2$ and in the potentials of the general form $V = \frac{1}{2}[\alpha(x^2 + y^2) + x^2y^2]$. We found that the stable period-9 periodic orbit of the YM potential belongs to a family of orbits that bifurcates from a basic period-9 family of the general form of the potential V, when α is slightly above zero. This basic period-9 family and its bifurcations exist only up to a maximum value of $\alpha = \alpha_{max}$. We calculate the Hénon stability index of these orbits. The pattern of the stability diagram is the same for all the symmetric orbits of odd periods 3,5,7,9 and 11, that we have found. We also found the stability diagrams for asymmetric orbits of period 2,3,4,5 which have again the same pattern. All these orbits are unstable for $\alpha = 0$ (YM potential) except for the stable orbits of period-9 and some orbits with multiples of 9 periods.

‡ Corresponding Author

1. Introduction

The Yang-Mills (YM hereafter) potential:

$$V = \frac{1}{2}x^2y^2 \tag{1}$$

is a simple potential that has attracted much interest because it was thought to be of Anosov type, thus it should not have any stable periodic orbits ([1], [2], [3], [4]). However, Dahlqvist and Russberg [5] (DR hereafter) have found a stable periodic orbit in this system, thus proving that the YM potential has both order and chaos and it is definitely not Anosov. In fact, because of the symmetries, there are also stable periodic orbits, formed by rotating the original orbit by 90^o, 180^o and 270^o (Fig.1). Moreover, every orbit can be described in two opposite directions (with opposite velocities) therefore there exist eight stable periodic orbits of the form found by DR. Of course there also exist higher order bifurcations from these families. In Fig. 1 we plot the curves of zero velocity (CZV with equation $y = \pm 1/x$) (black) inside which all orbits are limited. Note that the YM stable orbits come close to the zero velocity curves but they do not reach them.

The question whether chaos in Hamiltonian systems is complete or not was always of particular interest. Most systems have both ordered and chaotic orbits. However, if the non-periodic orbits are chaotic and fill the whole phase space, the system is called ergodic. If the filling is uniform the system is called mixing. If furthermore, the orbits have positive Kolmogorov entropy, the system is called Kolmogrov ([6], [7]). If finally in a Kolmogorov system the Lyapunov Characteristic Number LCN for all its orbits is between certain positive limits, i.e $0 < c_1 < LCN < c_2$, the system is called Anosov (for a review see [8], [9]). An Anosov system has infinite periodic orbits, but none of them is stable. Furthermore the Anosov systems are hyperbolic ([10]), i.e. at every point of an orbit the tangent space is decomposed into stable and unstable manifolds that intersect transversally.

The Anosov systems are structurally stable., i.e. a small perturbation of an Anosov system leads to another Anosov system.

A special class of Anosov systems are linear maps. An example is the cat map ([11]). It is easy to prove that this map is ergodic and mixing, and has positive Kolmogorov entropy. This mapping has infinite unstable periodic orbits.

Another class of linear systems that are not only ergodic, but also mixing, Kolmogorov and Anosov, is provided by the rational billiards ([12]). Billiards are closed systems with perfectly reflecting boundaries, where the motion of a particle is a straight line until it reaches the boundary and then it is reflected specularly. Such is the case of the stadium ([13]).

However, the mappings mentioned above, differ from generic dynamical systems which are non linear. If we add a nonlinear term in a linear mapping and if we have smooth reflections we see the appearance of islands around stable periodic orbits. Up to now, no 2D Hamiltonian system with a nonintegrable potential was found to be Anosov.

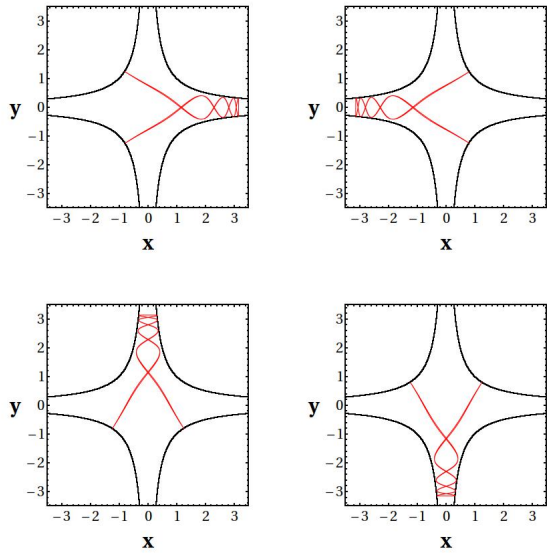

Figure 1. The period-9 stable periodic orbits of the potential (1) together with the curves of zero velocity.

The Yang Mills potential was thought to have only unstable periodic orbits. In fact, Sohos et al. in [4] studied the periodic orbits of an extented YM potential:

$$V = \frac{1}{2}x^2y^2 + \frac{\alpha}{2}(x^2 + y^2) \tag{2}$$

and found indications that all periodic orbits become unstable as the nonlinearity parameter α decreases and goes to zero.

The YM potential and its extensions are of interest in the theory of high energy physics ([14], [15], [16]). On the other hand, systems of interest in galactic dynamics have potentials of the form of eq. (2). where α is of order $O(1)$. Such a case was studied in [17] by using the potential $V' = \frac{1}{2}(x'^2 + y'^2) + \epsilon x'^2 y'^2$, which is equivalent to eq. (2) if we set $\alpha = 1/\sqrt{2\epsilon}$ and $x' = \sqrt{\alpha}x$, $y' = \sqrt{\alpha}y$. (But this paper was devoted only to the form of the asymptotic curves of the main unstable periodic orbits). Further extensions of the YM potential were considered by Dahlqvist and Russberg in [18] in the form $V = (x^2y^2)^{1/\alpha'}$ with $\alpha' > 1$ and $\alpha' < 1$, (but their main interest was the quantization of the orbits).

The question is now why the extended YM potential of eq. (2) gives a stable family when $\alpha = 0$. In order to answer this question we make a numerical study of the stability and the characteristic curves of the periodic orbits starting from the YM potential (with $\alpha = 0$ in eq. (2)) and extrapolate our calculations for the extended YM potential with small positive α. The first interesting result was that the stable family of periodic orbits found by DR in the YM potential is the bifurcation of another stable family which exists for $\alpha > 0$.

We call this family "basic" period-9 family of periodic orbits, because several other period-9 families bifurcate from it.

The second interesting result was that this stable family exists only up to $\alpha = \alpha_{max} \approx 16.8 \times 10^{-4}$ (a small value close to zero) and joins there an unstable periodic family of the same period at a tangent bifurcation. Thus the YM stable periodic orbit cannot be joined by successive bifurcations with any family of periodic orbits that exist for large α (of order $O(1)$).

Finally, we find that the pattern of the stability curves of several symmetric and asymmetric periodic orbits of various periods and of their bifurcations is very similar to the pattern of the period-9 orbits. All these families terminate at a maximum value of α by tangent bifurcations with unstable orbits of the same period.

In the present paper we study the periodic orbits of the potential (2) for small values of α (near zero) and find their stability and their bifurcations. The energy is identified with the Hamiltonian :

$$H = \frac{1}{2}(\dot{x}^2 + \dot{y}^2) + \frac{1}{2}x^2y^2 + \frac{\alpha}{2}(x^2 + y^2) = E \tag{3}$$

In our study we take $E = 1/2$ for the total energy (as done by Dahlqvist and Russberg in [5]).

The paper is structured as follows: In section 2 we describe the periodic orbits found in the YM potential. In section 3 we find the stability and the characteristic curves of the periodic orbits of the generalized Hamiltonian (3) as a function of the parameter α. In section 4 we find new families of periodic orbits for values of α close to zero. Finally in section 5 we draw our conclusions.

2. Periodic orbits of the YM potential

The stable periodic orbit found by DR was considered by them to be of period 11, by counting the intersections with the axes $x = 0$ and $y = 0$ and with the line $x = y$. However, if we count only the intersections with the axis $y = 0$ going upwards (i.e. with $\dot{y} > 0$) we must consider this periodic orbit as of period-9. The initial conditions of this orbit, in the context of the precision we demand from our numerical calculations, are (x_0=3.14640122769753, $\dot{x}_0$ =0.0017931934191, y_0=0, $\dot{y}_0$=0.99999839222738. The desired precision here is of the order of 14 decimal digits). If we take for initial conditions (x_0'=x_0, y_0'=y_0, $\dot{x}_0'$=$-\dot{x}_0$, $\dot{y}_0'$=$-\dot{y}_0$) we have exactly the same periodic orbit described in the opposite direction. In Fig. 2a the Poincaré surface of section ((x, $\dot{x}$), for $y = 0$ and $\dot{y} > 0$) of the stable period-9 orbit is plotted for the YM potential and the order of the successive iterations is marked with numbers. There exists a second stable period-9 orbit (not plotted here) which is symmetric to the first one with respect to the axis $\dot{x} = 0$.

Apart from the two stable period-9 orbits, there are ten more unstable period-9 orbits in the YM potential shown in a zoom of the Poincaré surface of section around the value $\dot{x} = 0$ (in black, blue, magenta and orange in Fig. 2b). The black, blue and magenta period-9 orbits (shown in Fig. 2b) intersect the $x - axis$ perpendicularly (with $\dot{x} = 0$) at their maximum $x = x_{max}$. The orange period-9 orbits do not intersect

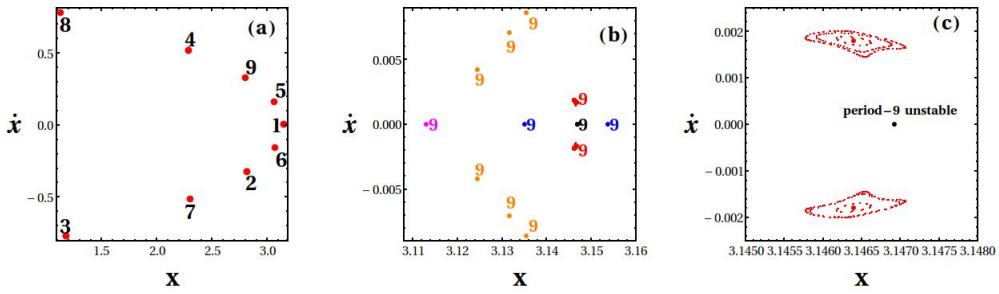

Figure 2. The Poincaré surface of section $(x, \dot{x})$ for $y = 0$ and $\dot{y} > 0$ for the YM potential. (a) A stable period-9 orbit. The order of the successive iterations is marked with numbers. (b) A zoom in of the phase space around $\dot{x} = 0$ where 12 period-9 orbits of the YM potential are marked. (c) A greater zoom in of the phase space focused only on the stable period-9 orbits and the surrounding invariant curves (red) as well as on the basic unstable period-9 (black) orbit. In this figure, red color denotes stability

.

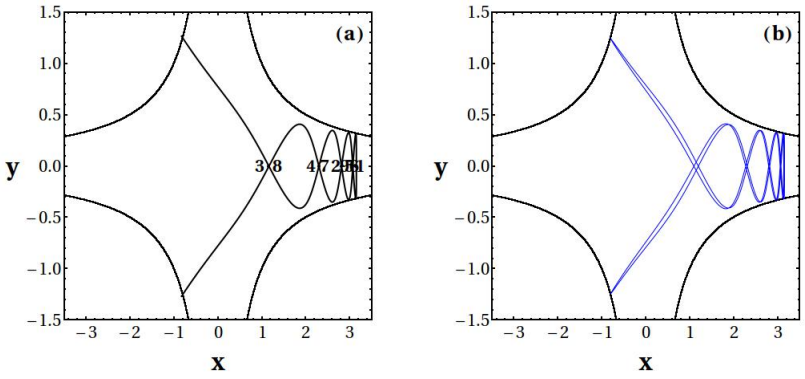

Figure 3. Two period-9 orbits of the YM potential. (a) The basic unstable period-9 orbit (black). The order of intersection of the trajectory by the x-axis upwards is shown in numbers. (b) One of the two unstable period-9 orbits (blue) bifurcated from the basic one. The colors of the orbits are the same as their corresponding points on the phase space in Fig. 2b.

the $x - axis$ perpendicularly at their maximum $x = x_{max}$, but they have $\dot{x}_{x_{max}} > 0$ or $\dot{x}'_{x_{max}} < 0$, with $\dot{x}_{x_{max}}$ and $\dot{x}'_{x_{max}}$ symmetrical about the axis $\dot{x} = 0$.

The red, blue, magenta and orange period-9 orbits are bifurcated from the basic (black) period-9 orbit for values of $\alpha \neq 0$ in the generalized Hamiltonian (3), as we will show below. In Fig 2c a greater zoom in of the phase space is focused only around the stable period-9 orbits. These orbits are surrounded by sets of invariant curves (islands of stability). Every island consists of invariant curves and among them there are high order stable and unstable periodic orbits with periods multiples of 9. Around the islands of stability there is chaos. In Fig. 2 red color denotes stability.

In Fig. 3a we plot the basic unstable period-9 orbit (black) for $\alpha = 0$. The order

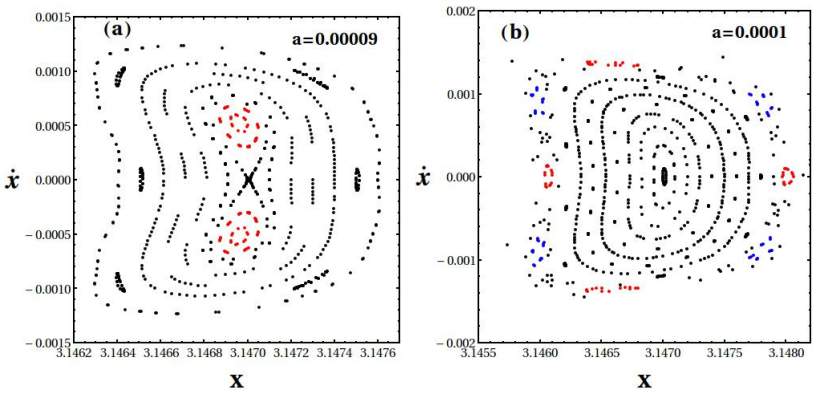

Figure 4. A zoom in of the Poincaré surface of section $(x, \dot{x})$, for $y = 0$ and $\dot{y} > 0$ (a) for $\alpha = 0.00009$. The basic period-9 periodic orbit is unstable (black). The red islands of stability correspond to the two stable period-9 periodic orbits bifurcated from the basic one. (b) for $\alpha = 0.0001$. The basic period-9 periodic orbit is stable. Two stable period-36 orbits are marked in blue and red around the basic period-9 orbit.

of intersection of the trajectory by the x-axis upwards is shown in numbers. The orbit forms 4 loops and its maximum x intersects perpendicularly the x-axis. It is reflected on the CZV at two points and returns through exactly the same path. In Fig 3b one of the two unstable period-9 orbits (blue), bifurcated from the basic one (see Figs. 5, 6 below) is plotted. This orbit is not reflected back to the same path, but after reaching the farthest point on the left, close to the CZV, it returns along a slightly different path. The colors of the orbits are the same with their corresponding points on the phase space in Fig. 2b. All these period-9 orbits are symmetric with respect to the $y = 0$-axis and form 4 loops.

When α increases slightly above $\alpha = 0$ in Hamiltonian (3) the two islands of stability of Fig. 2c approach each other and come close to the basic unstable periodic orbit. In Fig. 4a we plot the Poincaré surface of section for $\alpha = 0.9 \times 10^{-4}$. The red islands of stability correspond to the two stable period-9 periodic orbits bifurcated from the basic one. There are invariant curves surrounding both islands of stability. In Fig. 4b we plot the Poincaré surface of section for $\alpha = 10^{-4}$. The two islands of stability of Fig. 4a have joined into one island around the basic period-9 family which has become now stable. Around the basic stable periodic orbit there are higher order islands of stability.

3. Stability of the periodic orbits

The stability of the periodic orbits is found by calculating the Hénon stability index HI ([19], see also [9]). This is related to the eigenvalues $\lambda_{1,2}$ of the periodic orbit by the relation (see Appendix):

$$\lambda_{1,2} = HI \pm \sqrt{(HI)^2 - 1} \tag{4}$$

The orbit is stable if $|HI| < 1$ and unstable if $|HI| > 1$. In the Appendix we explain, in detail, the method of finding the periodic orbits as well as their Hénon stability indices.

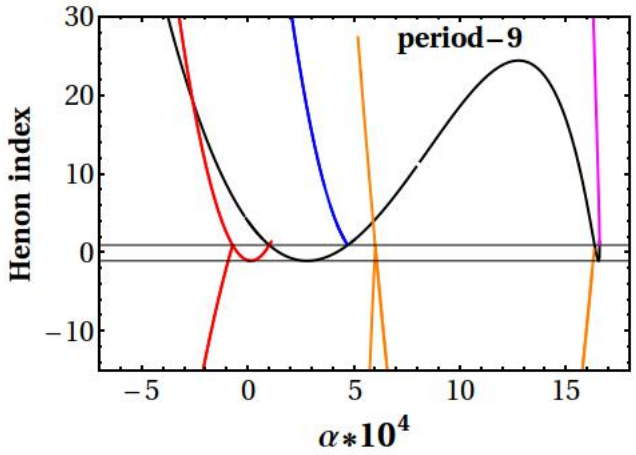

Figure 5. The HI as a function of the parameter α of the Hamiltonian (3) for the period-9 orbits.

The stability curve ($HI = F(\alpha)$) of the basic period-9 orbit is given in Fig. 5 (black). This orbit is stable in some small intervals of α. It disappears at a maximum $\alpha = \alpha_{max} \approx 16.8 \times 10^{-4}$, having $HI = +1$, where it joins another period-9 orbit (magenta) at a tangent bifurcation. This last period-9 orbit exists for $\alpha < \alpha_{max}$ and it is always unstable.

In order to plot this stability diagram we use the following procedure: We take the stable periodic orbit $(x_0, \dot{x_0})$ found by DR for $\alpha = 0$ (plotted in red in Fig. 5) and with the use of the Newton-Raphson method (described in the Appendix) we extrapolate the values of the periodic orbits, together with their HIs, for small values of α greater than zero, as well as for negative values of α . Each time the stability curve crosses the value $HI = \pm 1$, a new periodic orbit is generated, for decreasing values of α, with equal period (for $HI = +1$), or with double period (for $HI = -1$).

Each time the HI curve of the basic period-9 orbit crosses the $HI = +1$ axis from stability to instability (as α decreases) two orbits of the same period (9) are bifurcated from it. The stability curves of these bifurcations are shown in orange and red. The corresponding orbits are stable close to the bifurcation point and then (by decreasing α) they reach a minimum value of HI. The minimum of the red curve is on the axis $HI = -1$. For $\alpha = 0$ (YM potential) the HI of the red curve is a little greater than -1 and so the period-9 orbits (corresponding to the red branch of the stability curve) are stable. When their HI curves cross again the axis $HI = +1$ (for small negative α), two more stable orbits of the same period (9) are bifurcated that become unstable for smaller α and never again become stable. A similar pattern is formed by the HI curves of the orange families. However, the orbits of these families are unstable for $\alpha = 0$.

On the other hand, when the HI curve of the basic period-9 orbit crosses the $HI = +1$ axis from instability to stability (as α decreases) two orbits of the same

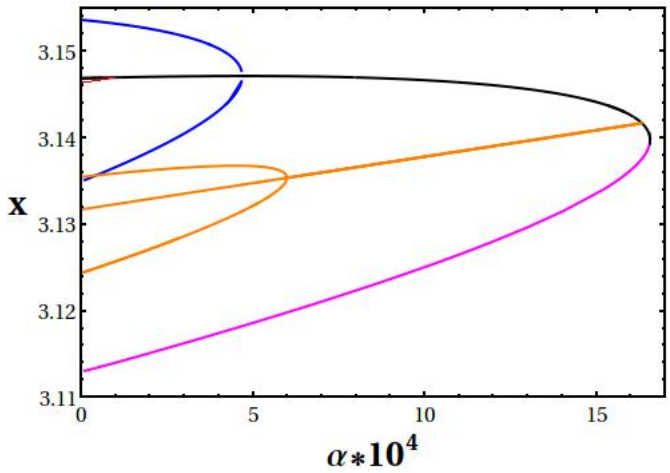

Figure 6. The characteristics $x = F(\alpha)$ of all the period-9 family of orbits.

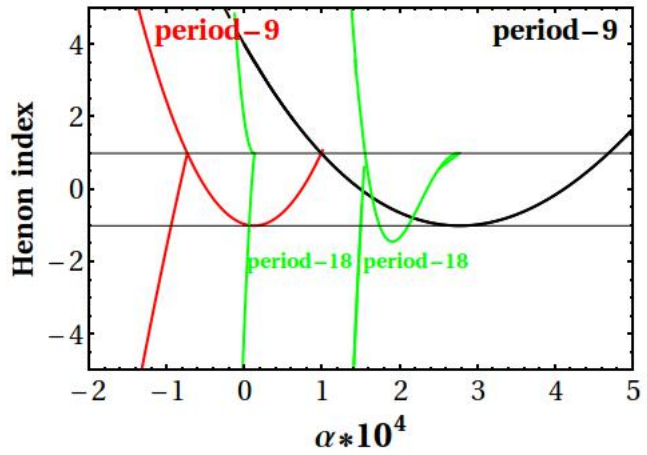

Figure 7. The HI as a fuction of the paremeter α of three period-9 families (one black and two red) and of some period-18 bifurcations (green).

period (9) are bifurcated from it (blue curve) which are always unstable for smaller values of α.

The characteristics ($x = F(\alpha)$) of the various families of period-9 orbits are shown in Fig.6. We follow the same color notation as in Fig. 5. We notice that there is only one unstable period-9 orbit (magenta) having a tangent bifurcation with the basic one. In Fig. 6 we see only one small red curve (corresponding to the stable periodic orbit of the YM potential), but there is also another one with the same x and symmetric $\dot{x}$ (Fig. 2b).

Finally there are six more (orange) period-9 orbits. Two of them bifurcate from the basic period-9 orbit and four more bifurcate from the first two. We see the three of them in Fig.6 and there are three more with the same x and symmetric $\dot{x}$. The red

and orange period-9 bifurcations do not intersect perpendicularly the x-axis near their maximum $x = x_{max}$, but they form families with $\dot{x} > 0$ and symmetric ones with $\dot{x} < 0$ (see Fig. 2b).

Besides the period-9 periodic orbits we have also period-18 bifurcations, each time the period-9 stability curves cross the $HI = -1$ axis or become tangent to it. Some examples are shown in Fig. 7. For $\alpha = 0$ (YM potential) these orbits are unstable.

4. Other families of orbits for the generalized YM potential

As we can see in Fig.3a, the basic period-9 periodic orbit (black) reaches the CZV and returns along the same path. The equation of the CZV, for $\alpha = 0$, is given by the relations $yx = \pm 1$, while for $\alpha \neq 0$ it is given as follows:

$$y = \frac{\pm\sqrt{\Delta}}{2(\alpha + x^2)}, \qquad \Delta = -4(\alpha + x^2)(\alpha x^2 - 1) \tag{5}$$

We have tried to find periodic orbits of various multiplicities, by taking initial conditions

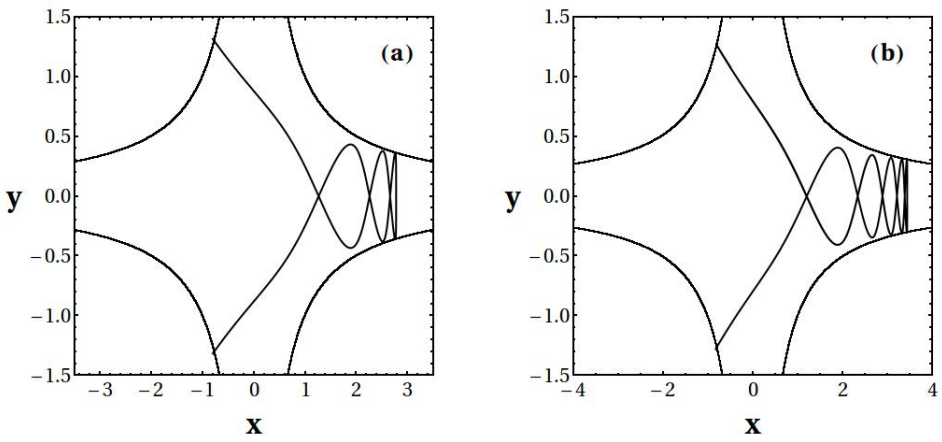

Figure 8. (a) The unstable period-7 periodic orbit for $\alpha = 0$ (b) The unstable period-11 periodic orbit for $\alpha = -0.008$.

along the CZV. The method we use is the following: By taking several initial conditions (x, y) along the CZV of the upper left quarter we find orbits that are reflected there and intersect almost perpendicularly the $x - axis$ at their maximum $x = x_{max}$. In such a way we find orbits that form fewer or more loops than the period-9 orbit. We take as initial guesses the values $(x_{max}, \dot{y}_{x_{max}})$ of these orbits and we set also $\dot{x} = y = 0$. Then by using the Newton-Raphson method as explained in the Appendix we find the initial conditions of the periodic orbits, in the context of the precision we demand from our numerical calculations on the Poincaré surface of section $(x_0, \dot{x_0} = 0, y_0 = 0, \dot{y_0})$ and then by integrating these initial conditions we plot the periodic orbit on the (x, y) configuration space. The periodic orbits that we found in this way, for $\alpha = 0$, are all unstable.

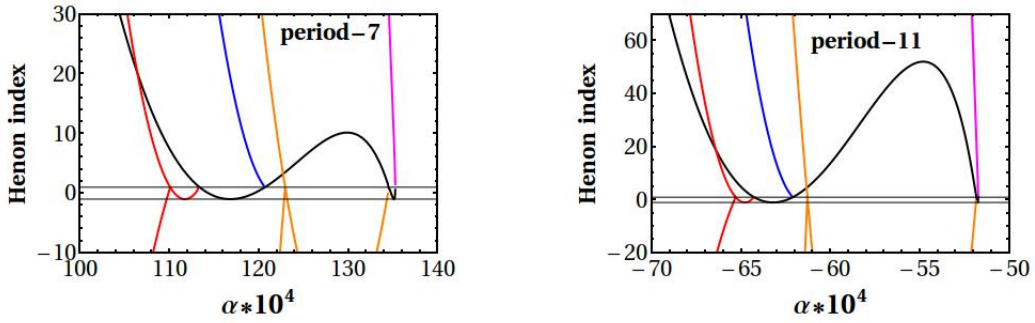

Figure 9. The HI as a function of the parameter α of the Hamiltonian (3) for the period-7, and period-11 periodic orbits.

Using the method described above we find a period-7 periodic orbit for $\alpha = 0$ (Fig. 8a) and a period-11 periodic orbit for $\alpha = -0.008$ (fig. 8b). The period-7 orbit is similar to the period-9 orbit (Fig. 3a), but has fewer loops (3) around the $y = 0$ axis. On the other hand, the period-11 orbit has more loops (5) than the period-9 orbit.

We plot the HI of the period-7 families as functions of the parameter α in Fig.9a and the HI of the period-11 families in Fig. 9b. We observe that the basic period-7 and period-11 families (black) as well as all their bifurcations follow the same pattern as the period-9 families of orbits (compare with Fig. 5). The only difference is that the basic period-7 family and its bifurcations are stable for values of α larger than the ones of the period-9 family, and the period-11 family and its bifurcations are stable for negative values of α. These figures indicate that the same pattern of the $HI = F(\alpha)$ curves is repeated for all the odd period periodic orbits (period-5 and 3 for positive and larger values of α and periods larger than 11 for negative values of α).

By taking initial conditions along the CZV curve for various values of α we have also found, using the method described above, some asymmetric orbits (with initial conditions $x_0 = x_{max}, y_0 = 0,\ \dot{x_0} \neq 0, \dot{y_0} \neq 0$) of various periods, using again the Newton-Raphson method (see Appendix). These orbits do not intersect the $x - axis$ perpendicularly at their maximum $x = x_{max}$. The notion "asymmetric" here means that the orbits are not symmetric with respect to the $y = 0$-axis, in contrast with the orbits of Figs. 3,8. In Figure 10 asymmetric orbits with periods 5,4,3,2 are plotted. These orbits are reflected on the CZV at one point on the left and one point on the right and return through exactly the same path. The corresponding HI diagrams as functions of the parameter α of these orbits are shown in Fig. 11. We observe that they all follow the same pattern, but for different ranges of the parameter α.The asymmetric period-5 family of orbits found here exists only for negative values of the parameter α.

All the families of orbits of Fig. 11, disappear with a tangent bifurcation at a maximum $\alpha = \alpha_{max}$ and they have one bifurcation of a family of the same period (green curve) for smaller values of α. These families are all unstable for $\alpha = 0$ (YM potential).

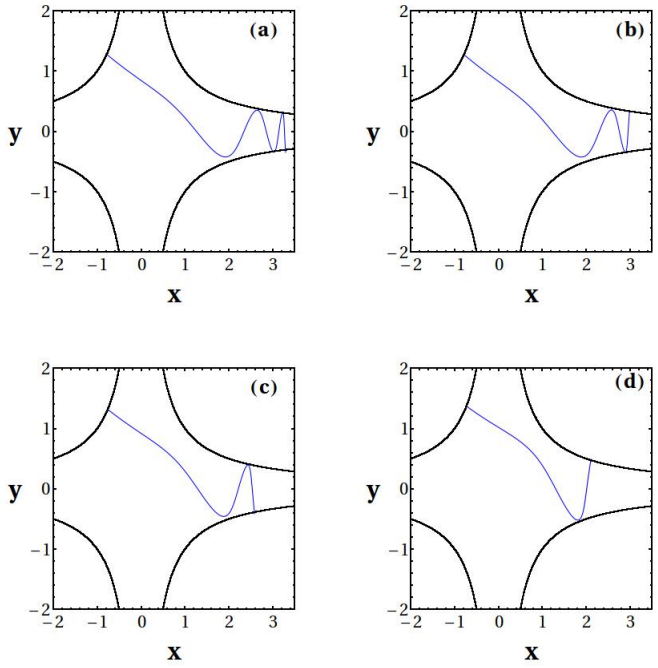

Figure 10. The asymmetric orbits of (a) period-5 for $\alpha = -0.008$ (b) period-4 for $\alpha = 0$ (c) period-3 for $\alpha = 0$ and (d) period-2 for $\alpha = 0$ with the corresponding CZVs.

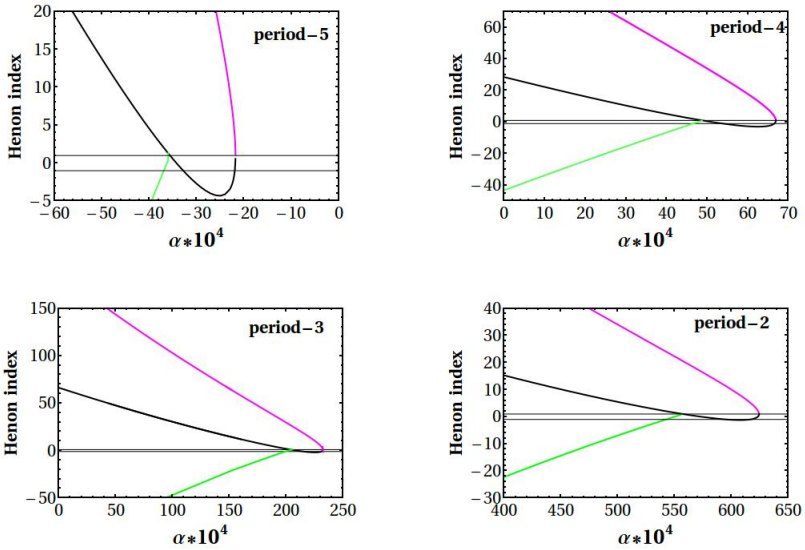

Figure 11. The HIs as functions of the parameter α of the asymmetric orbits of period 5,4,3,2 (black curves) together with their bifurcations. They all follow the same pattern and they disappear with a tangent bifurcation at a maximum $\alpha = \alpha_{max}$ with an unstable family of the same period (magenta).

5. Conclusions

In the present paper we made a numerical study of the orbits (and their stability) in potentials of the form $V = \frac{\alpha}{2}(x^2+y^2)+\frac{1}{2}x^2y^2$, with α close to zero, which is a generalized potential of the Yang-Mills (YM) potential $V = \frac{1}{2}x^2y^2$.

We found a number of period-9 periodic orbits (intersecting the x-axis 9 times upwards, with $\dot{y} > 0$) by using the Newton-Raphson method described in the Appendix. In the YM potential we have found that there are at least 8 stable period-9 orbits. But close to every stable orbit there exist 10 more unstable period-9 orbits.

All these period-9 orbits are bifurcations of a basic period-9 family. This basic period-9 family is terminated at a tangent bifurcation with an unstable period-9 family, at a maximum $\alpha = \alpha_{max} = 16.8 \times 10^{-4}$ and having there Hénon index $HI = +1$. Thus, all these period-9 families do not extend to large values of α of order $O(1)$.

The various period-9 bifurcations of the basic periodic orbit are generated when the HI of this orbit intersects the $HI = +1$ axis. We give the characteristics ($x = F(\alpha)$) of the various bifurcating families.

We had also found periodic orbits of other multiplicities. We gave the HI stability curves of the period-7 and period-11 periodic orbits which have the same pattern as the HI stability curve of the period-9 orbits, but they are displaced in the values of α. We have found that the smaller the period of the orbit the larger the value of α for which it is terminated at a tangent bifurcation. These stability curves indicate that all the periodic families of odd periods (and intersecting perpendicularly the $x-$ axis) have the same pattern together with their bifurcations. The periodic orbits having period 11 or larger exist only for negative values of α while the period-9,7,5 and 3 periodic orbits are terminated at positive values of α. All these periodic orbits that we have found are unstable for $\alpha = 0$ (YM potential) except for the stable bifurcation of the basic period-9 orbit found by DR in [5].

Furthermore, we have found some asymmetric periodic orbits (the notion "asymmetric" means that the orbits are not symmetric with respect to the $y = 0$-axis) of periods 2,3,4 and 5 (that do not intersect perpendicularly the x-axis at their maximum $x = x_{max}$). These orbits have two limiting points on the curves of zero velocity (CZV) and reach a maximum value of α where they are terminated at a tangent bifurcation with an unstable periodic orbit of the same period. They have all the same pattern of stability curves, together with their bifurcations.

We conclude that the stability patterns seem to be quite general in the case of a near YM potential both in the case of symmetric and asymmetric periodic orbits. All these orbits are unstable at the value $\alpha = 0$ (YM potential).

We did not find any stable periodic orbits in the YM potential except for the stable period-9 family and its higher order bifurcations with periods multiples of 9. However, the question of whether there exist other stable periodic orbits in the YM potential is still open.

References

[1] Savvidy, G. K. (1983), Phys. Lett., B130, 303.
[2] Savvidy, G. K. (1984), Nucl. Phys., B246, 302.
[3] Carnegie A. and Percival I. C. (1984), J. Phys. A, 17, 801.
[4] Sohos G., Bountis T. and Polymilis H. (1989), Nuovo Cimento, B104, 339.
[5] Dahlqvist P. and Russberg G. (1990), Phys. Rep. Lett., 65, 2837.
[6] Kolmogorov A.N., (1958), Dokl. Akad. Nauk. SSSR 119, 861
[7] Sinai, Ya. G., (1976), Introduction to Ergodic Theory, Princeton Univ. Press, Princeton.
[8] Liverani C. and Wojtkowski M. P., (1995), "Dynamics Reported, Exposistions in Dynamical Systems", Jones C., Kirchgraber U. and Walther (eds.), 4, 130, Springer, Berlin.
[9] Contopoulos G., (2002) "Order and chaos in dynamical astronomy", Springer, Berlin.
[10] Guckenheimer, J. and Holmes , P., (1983), Noninear Oscillations, Dynamical Systems and bifurcations of Vector Fields, Springer, New York.
[11] Arnold, V.I. and Avez, A. (1968), "Ergodic Problems of Classical Mechanics", Benjamin, New York.
[12] Eckhardt, B, Ford, J. and Vivaldi, F (1984), Physica D, 13, 339.
[13] Bunimovich, L.A. (1979). "On the Ergodic Properties of Nowhere Dispersing Billiards". Commun. Math Phys., 65, 295.
[14] de Wit B., Hoppe J. and Nicolai H. (1988), Nucl.Phys., B305, 545.
[15] de Wit B, Luscher M. and Nicolai H. (1989), Nucl.Phys., B320, 135.
[16] Axenides M., Floratos E. and Linardopoulos G., (2017), Phys.Lett., B773, 265.
[17] Contopoulos G., Papadaki H. and Polymilis C. (1994), Cel. Mech. Dyn. Astron., 60, 249.
[18] Dahlqvist P. and Russberg G. (1991), J. Phys. A., 24, 4763.
[19] Hénon, M. (1965), Ann. Astrophys., 28, 992.

Appendix A. Determining periodic orbits and Hénon stability indices

All the periodic orbits of this study are found with the use of Newton-Raphson method, on the Poincaré surfaces of section $(x, \dot{x})$, for $y = 0$ and $\dot{y} > 0$. The image of an initial point $(x_0, \dot{x_0})$ in a 2D mapping is given, in general, by analytical functions:

$$x_0' = f(x_0, \dot{x_0}, \alpha), \qquad \dot{x_0}' = g(x_0, \dot{x_0}, \alpha) \tag{A.1}$$

where α is the nonlinearity parameter.

In the case of Hamiltonian systems, where the functions f, g are unknown, the iterations on the Poincaré surfaces of section are found numerically by integrating the orbit with initial conditions $(x_0, \dot{x_0})$ through the Hamilton equations:

$$\frac{dx}{dt} = \frac{\partial H}{\partial \dot{x}}, \quad \frac{d\dot{x}}{dt} = -\frac{\partial H}{\partial x} \tag{A.2}$$

We use the *Mathematica software system, the NDsolve command and the Automaticmethod for solving the differential equations (A.2) and find the next point* $(x_0', \dot{x_0}')$, *with* $y = 0$ *and* $\dot{y} > 0$ *and the required accuracy.*

In order to find a stable periodic orbit, with a given multiplicity on the Poincaré surface of section (and with a certain accuracy), we give an initial guess $(x_0, \dot{x_0})$ *(selected*

with the help of the Poincaré surface of section, close to the center of an island of stability). Then we use an iterative Newton-Raphson method to find the position of the periodic orbit, in the context of the precision we demand from our numerical calculations.

In order to study the stability of a periodic orbit $(x_0, \dot{x}_0)$ *we make linearization around it, given by the equation:* $\dot{\xi} = M\xi$ *, where* ξ *is a small deviation from the periodic orbit.* M *is the monodromy matrix of the system given by the relation:*

$$M = \begin{bmatrix} a_{11} & a_{12} \\ a_{21} & a_{22} \end{bmatrix} \tag{A.3}$$

where

$$a_{11} = \frac{\partial f}{\partial x_0}, \quad a_{12} = \frac{\partial f}{\partial \dot{x_0}}, \quad a_{21} = \frac{\partial g}{\partial x_0}, \quad a_{22} = \frac{\partial g}{\partial \dot{x_0}} \tag{A.4}$$

In the case of Hamiltonian systems, we calculate numerically the derivatives of eqs. (A.4). We symbolize with $(x_0', \dot{x_0}')$*=Poinc*$(x_0, \dot{x_0})$ *the first iteration (or the* n^{th} *iteration if the periodic orbit is of multiplicity* n*) of the initial point* $(x_0, \dot{x_0})$*, which is an initial guess of the periodic orbit, on the surface of section* $(x_0, \dot{x_0})$*, for* $y = 0$ *and* $\dot{y} > 0$*. Then, we can construct the derivatives of eqs. (A.4) as follows:*

We first make the following mappings:

$$\begin{aligned} (x_{0_{11}}, \dot{x_{011}}) &= Poinc(x_0 + dx_0, \dot{x_0}) \\ (x_{0_{12}}, \dot{x_{012}}) &= Poinc(x_0 - dx_0, \dot{x_0}) \\ (x_{0_{21}}, \dot{x_{021}}) &= Poinc(x_0, \dot{x_0} + d\dot{x_0}) \\ (x_{0_{22}}, \dot{x_{022}}) &= Poinc(x_0, \dot{x_0} - d\dot{x_0}) \end{aligned} \tag{A.5}$$

where dx_0 *and* $d\dot{x_0}$ *are small deviations of the initial values* x_0 *and* $\dot{x_0}$*. Then, the derivatives of eqs. (A.4) are found approximately as follows:*

$$\begin{aligned} a_{11} &= \frac{\partial f}{\partial x_0} = \frac{x_{0_{11}} - x_{0_{12}}}{2dx_0}, \qquad a_{12} = \frac{\partial f}{\partial \dot{x_0}} = \frac{x_{0_{21}} - x_{0_{22}}}{2dx_0} \\ a_{21} &= \frac{\partial g}{\partial x_0} = \frac{\dot{x_{0_{11}}} - \dot{x_{0_{12}}}}{2d\dot{x_0}}, \qquad a_{22} = \frac{\partial g}{\partial \dot{x_0}} = \frac{\dot{x_{0_{21}}} - \dot{x_{0_{22}}}}{2d\dot{x_0}} \end{aligned} \tag{A.6}$$

Then we introduce the matrix:

$$I = \begin{bmatrix} a_{11}' & a_{12}' \\ a_{21}' & a_{22}' \end{bmatrix} = \begin{bmatrix} a_{11} - 1 & a_{12} \\ a_{21} & a_{22} - 1 \end{bmatrix}^{-1} \tag{A.7}$$

and according to the Newton-Raphson method the first approach to the periodic orbit is given by the relation:

$$\begin{aligned} x_{0_1} &= x_0 - [(x_0' - x_0).a_{11}' + (\dot{x_0}' - \dot{x_0}).a_{12}'] \\ \dot{x_{0_1}} &= \dot{x_0} - [(x_0' - x_0).a_{21}' + (\dot{x_0}' - \dot{x_0}).a_{22}'] \end{aligned} \tag{A.8}$$

By setting now $(x_{0_1}, \dot{x_{0_1}})$ *as the new initial guess of the periodic orbit we repeat the previous procedure of eqs. (A.5)-(A.8). In general, we repeat the same procedure* k

times until after the k^{th} iteration we get the required accuracy $|x_{0_k}\text{-}\ x_{0_{k-1}}| \leq acc$. In our calculations of the periodic orbits we require $acc \leq 10^{-10}$.

Once we have found the periodic orbit $(x_0, \dot{x_0})$ with the required accuracy, we can easily determine its Hénon stability index HI.

by the equation:

$$\begin{vmatrix} a_{11} - \lambda & a_{12} \\ a_{21} & a_{22} - \lambda \end{vmatrix} = 0 \tag{A.9}$$

By solving eq. (A.9) we get the 2 eigenvalues λ_1, λ_2 of the periodic orbit:

$$(a_{11} - \lambda).(a_{22} - \lambda) - a_{12}.a_{21} = 0 \tag{A.10}$$

The conservation of areas implies that the determinant of the matrix (A.3) is equal to unity and thus, eq. (A.10) finally becomes:

$$\lambda^2 - (a_{11} + a_{22})\lambda + 1 = 0 \tag{A.11}$$

The eigenvalues $\lambda_{1,2}$ are related to the Hénon stability index HI through eq. (3) of section 3 and thus:

$$HI = \frac{a_{11} + a_{22}}{2} \tag{A.12}$$

Therefore, we can determine if the periodic orbit is stable (if $|HI| < 1$) or unstable (if $|HI| > 1$).

In order to find an unstable periodic orbit we use as initial guess value (x_0, $\dot{x_0}$) a value close to the one of the periodic orbit from which it bifurcates, (for a value of α close to the bifurcating point) and then we find the value of the periodic orbit, in the context of the precision we demand from our numerical calculations, using the Newton-Raphson method described above.

Once we have found a periodic orbit for a given parameter α (see eq. (3)) we can easily find its characteristic curve $x = F(\alpha)$ (Fig. 6) and its HI stability curve $HI = F(\alpha)$ (figs. 5,7,9,11). Namely, if $(x_0, \dot{x_0})_i$ is the periodic orbit found for $\alpha = \alpha_i$ then we fix a small deviation $d\alpha$ and we use the Newton-Raphson method described above in order to find the corresponding periodic orbit $(x_0, \dot{x_0})_{i+1}$ for the value $\alpha_{i+1} = \alpha_i + d\alpha$, using as initial guess the value of the periodic orbit $(x_0, \dot{x_0})_i$. With this iterative method we can find the stability and the characteristic diagrams for any range of values of the parameter α.